Lipidomic Analysis of *C. elegans* Parkinson's Disease Models

A Major Qualifying Project Report:
Submitted to the Faculty of
WORCESTER POLYTECHNIC INSTITUTE
In partial fulfillment of the requirements for the
Degree of Bachelor of Science
by

Kathleen Donovan
Biochemistry

Submitted: May 6th, 2021

Approved by:
Carissa Olsen, PhD
Chemistry & Biochemistry

Abstract

Parkinson's disease (PD), the second most common neurodegenerative disease, lacks a diagnostic biomarker or disease-modifying treatment. Altered lipids have been connected to PD, but their precise role in the disease is unknown. Here, we probed the phospholipid composition of PD models using RNAi knockdown of 6 familial PD genes in *C. elegans* followed by mass spectrometry. This analysis revealed a trend towards increased phosphatidylethanolamine (PE) species after knockdown of *unc-26*, the ortholog of human *PARK20*. Subsequent analysis of *unc-26* mutants substantiated this result, as a significant PE increase was observed. We conclude that lipids changes may be a viable diagnostic biomarker or therapeutic target for *PARK20*-related PD.

Table of Contents

Acknowledgements

Introduction

Parkinson's disease (PD), the second most common neurodegenerative disease, is characterized by progressive loss of dopaminergic neurons accompanied with motor symptoms (Tysnes & Storstein, 2017). These motor symptoms can include resting tremor, rigidity, slowed movements, and diminished balance (Sinclair et al., 2021). By the time a patient presents with motor symptoms, they have often already permanently lost a substantial amount of neurons (Schneider & Alcalay, 2020), which necessitates the identification of a reliable biomarker so that PD can be diagnosed earlier. Additionally, although one can treat the motor symptoms, there is no cure or disease-modifying treatment available for PD.

We do not currently know the cause of PD, as 90-95% of PD cases are sporadic, with the other 5-10% of cases being familial (Tysnes & Storstein, 2017) and linked to 19 known genes (Xicoy, Wieringa, & Martens, 2019). Many cellular processes have been associated with PD, such as oxidative stress, endoplasmic reticulum stress, immune response, and endosomal-lysosomal function. All of these processes share a key feature in that they involve lipids (Xicoy, Wieringa, & Martens, 2019). In fact, single-nucleotide polymorphisms located in lipid metabolism genes have been correlated to sporadic PD (Xicoy, Wieringa, & Martens, 2019). Present studies of lipid changes in PD conflict depending on the sex, age, or PD etiology of a patient (Xicoy, Wieringa, & Martens, 2019). Although lipids seem to play a key role in PD, whether that role is pathological or compensatory is unclear (Xicoy, Wieringa, & Martens, 2019).

In this study, we sought to further characterize the role of lipids in PD by probing the phospholipidome of several *Caenorhabditis elegans* models of PD. We observed significant differences in phospholipid composition and trends towards altered phospholipid turnover in one of these models, the *unc-26* mutant. Further study is required to understand the molecular mechanisms leading to the phospholipid disruption observed. We propose that these alterations in phospholipid composition and turnover provide a viable therapeutic target for PD or a biomarker for diagnosis.

Background

1. Parkinson's Disease

Parkinson's disease (PD) is a progressive neurodegenerative disease, with its primary symptoms including muscle tremors and rigidity (Farmer et al., 2015). Non-motor symptoms of PD include depression, apathy, anxiety, dementia, disrupted sleep, constipation, and more (Cooper & Raamsdonk, 2018). In the human population above 60 years old, 1% of people are affected by PD, making it the second most common neurodegenerative disease (Xicoy, Wieringa, & Martens, 2019). In the coming two decades, the number of people with PD is proposed to double with the aging population (Nair et al., 2018). This prediction is daunting, since there is currently no cure for PD (Goya et al., 2020).

PD affects one of the brain's four major dopamine pathways: the nigrostriatal pathway (Farmer et al., 2015). Overtime in PD, there is loss of these dopaminergic neurons, as well accumulation of aggregates of the protein α-synuclein (α-syn), which are called Lewy bodies (Spillantini et al., 1998). α-syn aggregation has been observed to start in peripheral tissues, specifically the intestine, and gradually spread to multiple brain regions (Goya et al., 2020). Many cellular pathways have been found to be correlated to PD pathology, including oxidative stress, endosomal-lysosomal dysfunction, endoplasmic reticulum stress, and immune response (Xicoy, Wieringa, & Martens, 2019). PD can be familial, being caused by inheritance of a mutation, or sporadic. 5-10% of PD cases are familial, and thus far there are 19 known familial gene mutations associated with PD (Xicoy, Wieringa, & Martens, 2019).

Currently, the only conclusive diagnostic for PD is an assessment of the brain's dopaminergic neurons post-mortem, with 60-80% of neurons being depleted as the requirement for a positive diagnosis (Sinclair et al., 2021). A clinician can give an informal PD diagnosis based on the presence of one or more of the typical PD symptoms: bradykinesia (slowness of movement), resting tremor, rigidity, and postural imbalance (Sinclair et al., 2021). However, these diagnoses can be inaccurate. Recent studies have explored several potential diagnostic tests, including analyzing cerebrospinal fluid α-syn (Kang et al., 2019), profiling the gut microbiome (Nair et al., 2019), or probing the sebum metabolome (Sinclair et al., 2021). Yet, there is still a need for a widely accepted and reliable biomarker, so that PD patients can be accurately diagnosed earlier, and thus receive treatment earlier (Kang et al., 2019). Presently, by

the time motor phenotypes manifest, PD patients have already permanently lost a considerable number of neurons (Schneider & Alcalay, 2020).

There are several drugs to treat PD on the market, with most targeting the dopaminergic pathway specifically. While these treatments can help alleviate motor symptoms, there is not any evidence to suggest these treatments slow disease progression (Schneider & Alcalay, 2020). Clinical trials for disease-modifying PD drugs have failed in recent years, and Schneider & Alcalay suggest that this is possibly because these treatments are taking a "one-size-fits-all" approach (2020). Since each PD patient has a unique genotype, they suggest that future work needs to be done to design precision medicine-based treatments for PD (Schneider & Alcalay, 2020).

2. Membranes: Dynamic Lipid Boundaries

Between a cell and its environment, there is a 30 angstrom hydrophobic barrier: the membrane (van Meer, Voelker, & Feigenson, 2008). Membranes are composed primarily of a class of biomolecules known as lipids. Membrane lipids serve as a framework for membrane protein receptors, transporters, and enzymes (Sultana & Olsen, 2020). In eukaryotic cells, a significant portion (5%) of the cell's genes are used to synthesize lipids (van Meer, Voelker, & Feigenson, 2008). However, we do not know the specific biological roles of many of these lipids (van Meer, Voelker, & Feigenson, 2008). There are eight classes of lipid: fatty acyls, glycerolipids, glycerophospholipids, sphingolipids, sterols, prenol, saccharolipids, and polyketides (Xicoy, Wieringa, & Martens, 2019). The major lipid class found in eukaryotic cell membranes is glycerophospholipids (Sultanta & Olsen, 2020), herein referred to as 'phospholipids'. The specific distribution of phospholipids comprising the membrane ultimately changes the optimum packing and fluidity of the membrane, affecting cell function (Sultana & Olsen, 2020).

Cells must tightly regulate their membrane composition in order to optimize membrane function (Dancy et al. 2015). Membrane lipids are consumed by events such as vesicle trafficking, phospholipase activity, lysosomal degradation, and beta-oxidation (Sultana & Olsen, 2020). The correct lipids must be brought to the membrane continuously to replenish these consumed lipids during a process called lipid turnover (Sultana & Olsen, 2020). Also, the membrane composition must be changed in order to accommodate changes in the environment, such as temperature fluctuations (Sultana &

Olsen, 2020). Thus, membranes are not static barriers, but highly dynamic structures (Dancy et al., 2015).

Phospholipids are composed of a hydrophilic head group and two hydrophobic fatty acid (FA) tails (Figure 1) (van Meer, Voelker, & Feigenson, 2008). In membranes, phospholipids are arranged in a bilayer, with the head groups facing the intracellular and extracellular environment, and the tails facing in towards each other. The inclusion of different head groups and tails generates great structural diversity within these lipids. The most abundant class of phospholipids, with lipids containing a choline head group and an acyl (phosphatidyl-) linkage, is the phosphatidylcholine (PC) class. PCs have a cylindrical geometry, due to the similar diameter of the head group and the two tails, and can self-assemble into a planar bilayer (van Meer, Voelker, & Feigenson, 2008). Other major structural phospholipids include phosphatidylethanolamine (PE), phosphatidylserine (PS), phosphatidylinositol (PI), and phosphatidic acid (PA) (van Meer, Voelker, & Feigenson, 2008). PE species contain a small and polar head group, which leads to a conical geometry, and thus a curvature in membranes with PE species (van Meer, Voelker, & Feigenson, 2008).

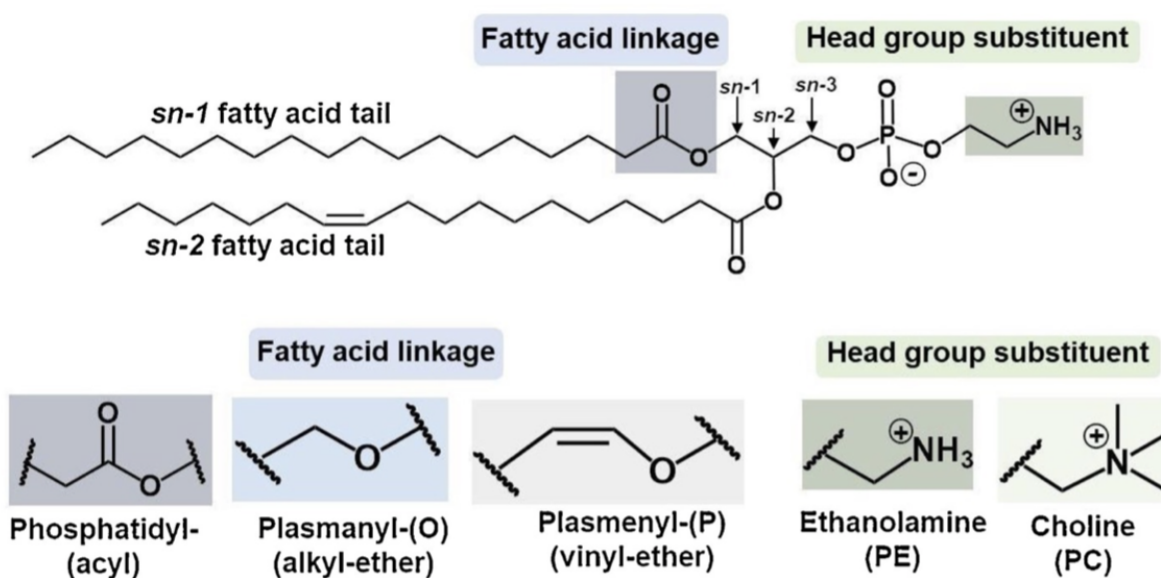**Figure 1. Phospholipid structure from Sultana & Olsen (2020).** Phospholipids (PLs) are composed of a hydrophilic head group and two hydrophobic fatty acid (FA) tails. There are several possible head groups, such as ethanolamine, or choline. The FA chains can vary in their length and saturation. Further diversity in the PL structure comes from the type of FA linkage: acyl, alkyl-ether, or vinyl-ether.

In addition to monitoring the composition of canonical phospholipids, there are also other membrane lipids that can be considered. For example, lyso lipids are produced from the hydrolysis of phospholipids and can act as messenger lipids. Lyso lipids, like lysophosphatidylcholine (LPC) and lysophosphatidylethanolamine (LPE) contain a single FA chain, and can therefore easily move laterally through membranes (Sultana & Olsen, 2020). This movement allows them to signal through interactions with membrane receptors (Sultana & Olsen, 2020).

Each class of phospholipid is not distributed evenly throughout membranes. Firstly, lipids can organize laterally into membrane domains which have distinct functions, such as recruiting proteins from the cytoplasm (van Meer, Voelker, & Feigenson, 2008). Also, certain lipids can be enriched in the inner or outer leaflet of a membrane—what is known as lipid asymmetry (van Meer, Voelker, & Feigenson, 2008). Typically, PS and PE species are enriched in the cytosolic leaflet of plasma and endosomal membranes (van Meer, Voelker, & Feigenson, 2008). One function of lipid asymmetry is that translocation of lipids to the cytosolic leaflet can contribute to budding by bending the membrane (van Meer, Voelker, & Feigenson, 2008).

3. Links Between Lipids and Parkinson's Disease

Recently, lipids have emerged as a central player in PD (Xicoy, Wieringa, & Martens, 2019). This connection makes sense, since the brain is highly lipid-rich, containing 50-60% lipid by dry weight (Hussain et al., 2019). Lipids are involved in several brain functions, such as impulse conduction, neurogenesis, insulation, and synaptogenesis (Hussain et al., 2019). Additionally, the brain requires lipids as an energy reserve (Hussain et al., 2019).

A specific connection of lipids to PD is that α-syn, the protein strongly implicated in PD, has been suggested to be a lipid-binding protein, interacting with phospholipids and FAs (Fanning, Selkoe, & Dettmer, 2020). In fact, a recent study found sphingomyelin and PCs to be present in Lewy bodies isolated from the tissue of PD brains (Shahmoradian et al., 2019). Additionally, excess membrane-associated α-syn can lead to an increase in monounsaturated FA abundance, which makes α-syn more neurotoxic by disrupting its homeostasis (Fanning, Selkoe, & Dettmer, 2020). Also of note is that single-nucleotide polymorphisms have been found in lipid metabolism genes (*SREBF1, DGKQ, ASAH1,* and *SMPD1*) in sporadic cases of PD (Xicoy, Wieringa, & Martens, 2019).

Lipid changes detected in PD patients can conflict based on the sex, age, and PD etiology of the patient, as well as the region of the body from which the sample came (Xicoy, Wieringa, & Martens, 2019). One common lipid change in PD patients is a build up of glucosylceramide caused by a heterozygous mutation in *GBA* (Fanning, Selkoe, & Dettmer, 2020). However, in *GBA* mutation carriers, while increased glucosylceramide can be detected in plasma, there is decreased or no change of these levels in the brain (Xicoy, Wieringa, & Martens, 2019). As far as phospholipids, total PE levels were detected to be decreased in the substantia nigra of PD patients prior to treatment, but PE levels in a different study were found to be increased in samples from frontal cortex lipid rafts (Xicoy, Wieringa, & Martens, 2019). Also, decreased levels of PCs containing polyunsaturated FAs has been seen in the frontal cortex of PD patients (Fanning, Selkoe, & Dettmer, 2020). Yet, in some studies, significant PC decreases were observed in male patients only (Fanning, Selkoe, & Dettmer, 2020).

Although it is clear that lipids are associated with PD, it has yet to be established whether lipids are playing a pathological or compensatory role in the disease (Xicoy, Wieringa, & Martens, 2019). This lack of understanding necessitates further research to define the role of lipids in PD. This work is particularly important because lipids could serve as a potential biomarker for PD (Hussain et al., 2019) or a supplementary therapeutic avenue. There is a precedence for using lipids as a therapeutic intervention in Alzheimer's disease (AD). Specifically, decreased levels of ethanolamine plasmalogens in plasma have been detected in AD patients, and were associated with cognition deficit and disease severity (Su, Wang, & Sinclair, 2019). Using plasmalogens as an intervention in AD patients and in rodents has shown a positive therapeutic effect in several studies (Su, Wang, & Sinclair, 2019).

4. Studying Lipids with Liquid Chromatography and Mass Spectrometry

Given that lipids are a chemically diverse group of molecules, they are challenging to study (Sultana & Olsen, 2020). Liquid chromatography tandem with mass spectrometry (LC-MS) is a widely used method to study cellular lipid composition (Cajka & FIehn, 2014). In this method, lipids first travel through a column, which separates the molecules based on their interactions with a solid and mobile phase. Typically, a reverse phase C_{18} silica column is used, which leads to molecules eluting in order of increasing hydrophobicity (Sultana & Olsen, 2020). After separation, molecules are then

subjected to mass spectrometry, which is able to identify individual lipids with great molecular specificity and detection sensitivity.

As mentioned in Section 2 above, membranes are highly dynamic structures. Thus, in addition to studying lipid composition, it is important to probe the turnover of lipids within the membrane. This type of study can be achieved by combining mass spectrometry with stable isotope labeling. Specifically, ^{15}N incorporation into phospholipid head groups has been used to investigate membrane lipid dynamics (Dancy et al., 2015).

5. *Caenorhabditis elegans*: a Model Organism

Caenorhabditis elegans is a soil nematode which is used to study neurobiology, development, apoptosis, cell signalling, cell cycle, cell polarity, gene regulation, metabolism, aging, and sex determination (Kaletta & Hengartner, 2006). This nematode can be used to study such a multitude of biological processes because *C. elegans* displays strong homology with humans in their cellular and molecular pathways (Kaletta & Hengartner, 2006). In fact, *C. elegans*' genome contains orthologs for 60-80% of human genes (Kaletta & Hengartner, 2006).

An additional benefit of using *C. elegans* in research settings is its rapid reproduction cycle—one nematode will produce about 300 offspring in one reproductive cycle, which takes about 3.5 days (Meneely, Dahlberg & Rose, 2019). *C. elegans* also have a lifespan of about three weeks, making aging studies more accessible. Additionally, *C. elegans'* small size lends itself to whole-animal high-throughput technologies (Kaletta & Hengartner, 2006). Finally, *C. elegans* can be easily and inexpensively maintained on agar plates seeded with the non-pathogenic *E. coli* strain OP50 (Meneely, Dahlberg & Rose, 2019).

Of particular importance is that, in contrast to cell culture systems, *C. elegans* eats and processes a diet as humans do. Thus, one can choose to study how diet, environmental conditions, and genetic background work together to influence cellular pathways. The nematode is also so small that one can enrich its diet with stable isotopes without an extremely high financial burden (Dancy et al., 2015). Finally, RNA interference (RNAi) libraries are readily available for *C. elegans*, making high-throughput genome-wide screens possible (Kaletta & Hengartner, 2006).

6. Modeling Parkinson's Disease in *C. elegans*

Due to the advantages discussed above, *C. elegans* are an extremely useful model organism for studying many human diseases. Relevant to study of neurodegenerative disease is the fact that *C. elegans*' nervous system is invariant and well characterized (Cooper & Raamsdonk, 2018). Neurons make up 302 of the 959 cells in the nematode, with all of the neurons having been mapped by electron micrographs (Cooper & Raamsdonk, 2018). There are numerous existing *C. elegans* models of neurological diseases, including PD. For example, there are transgenic nematodes which express α-syn or LRRK2, as well as nematodes with deletions in autosomal dominant PD genes (*PRKN/pdr-1, PINK1/pink-1, DJ-1/djr-1.1/djr-1.2 and ATP13A2/catp-6*) (Cooper & Raamsdonk, 2018).

In addition to these mutants, one can rapidly screen PD genes by knocking them down using the existing RNAi library for *C. elegans*. The RNAi, or RNA interference, technique works by the introduction of double-stranded RNA (dsRNA) causing specific inactivation of an endogenous gene of the same sequence (Kamath & Ahringer, 2003). RNAi is a critical tool for studying gene function, as it enables rapid and targeted gene knockdown (Kamath & Ahringer, 2003). In *C. elegans*, RNAi is accomplished by feeding the nematode bacteria that produce dsRNA (Kaletta & Hengartner, 2006). In contrast to mammalian systems, in *C. elegans* one can use long dsRNA, with 500-1,500 base pairs, as the nematode does not display nonspecific inhibition of protein synthesis through dsDNA-dependent protein kinases (Kaletta & Hengartner, 2006). While this method of gene silencing is effective for most tissues in *C. elegans*, previous work shows that neurons can be less sensitive to RNAi (Cooper & Raamsdonk, 2018).

To evaluate PD phenotypes in *C. elegans*, several assays exist. First, to assess dopaminergic neuron survival, one can express fluorescent proteins specifically in neurons with the dat-1 promoter (Cooper & Raamsdonk, 2018). Of course, locomotion is a relevant healthspan indicator in *C. elegans* when studying PD, as it indicates a disruption of dopamine signaling; this phenotype can be quantified by recording nematode movement through a stereomicroscope (Maulik et al., 2017). Compromised dopamine signaling also leads to basal slowing and increased ethanol preference (Cooper & Raamsdonk, 2018). Finally, fecundity, or ability to produce offspring, is controlled by dopamine in *C. elegans* (Maulik et al., 2017). Previous study of brood size in the *LRRK2* mutants showed that decreased levels of dopamine lead to decreased fecundity (Cooper & Raamsdonk, 2018).

When using *C. elegans* to study the link between PD and membrane lipids, one should note that *C. elegans*' membrane contains several differences to mammalian membranes. Specifically, *C. elegans* does not contain FA chains longer than 20 carbons, and does not utilize cholesterol to modify membrane fluidity (Sultana & Olsen, 2020). Although it is important to consider these differences, the lack of membrane cholesterol allows for the specific study of the role of phospholipids in PD.

7. Parkinson's Disease Genes of Interest

About 5-10% of PD cases are familial and can be linked to 19 genes (Xicoy, Wieringa, & Martens, 2019). In this study, we chose six of these genes in *C. elegans* which have orthologs to human PD genes: uncoordinated 26 (*unc-26*), cation transporting ATPase (*catp-6*), PTEN-induced kinase 1 (*pink-1*), leucine-rich repeat serine/threonine-protein kinase 1 (*lrk-1*), glutathione-independent glyoxalase 1.1 (*djr-1.1*), and sorbitol dehydrogenase 2 (*sodh-2*) (Table 1). The *catp-6, djr-1.1, lrk-1,* and *pink-1* genes were chosen specifically because they are established in *C. elegans* as models of PD (Cooper & Raamsdonk, 2018). We prioritized *unc-26*, as it is involved directly in modifying phosphoinositides, a type of signaling lipid (Ando et al., 2020). Finally, *sodh-2* was included because it is a less well-defined protein, but has been shown to correlate with α-syn aggregation when mutated (Knight et al., 2014), although it is not directly connected to PD.

Table 1. *C. elegans* orthologs to human PD genes investigated in this study.

C. elegans Gene	Human Ortholog & Type of PD	Type of Protein Encoded For	Gene Function	*C. elegans* Mutant Characteristics
unc-26	*SYNJ1/PARK20* Atypical early onset PD (Xie et al., 2019)	Phosphoinositide phosphatase (Ando et al., 2020)	Synaptic vesicle recycling, autophagosomal/ endosomal trafficking, phosphoinositide metabolism (Ando et al., 2020)	Small size, move backwards with jerky motion, and frequently coil (Todd et al., 2000)

catp-6	ATP12A3/ PARK9 Kufor Rakeb Syndrome (Anand et al., 2020)	Lysosomal transmembrane type 5 ATPase pump (Anand et al., 2020)	Lysosomal function (Anand et al., 2020)	Reduced thrashing, dysregulated iron metabolism, defective mitochondrial function (Anand et al., 2020)
pink-1	PINK1/PARK6 Autosomal recessive early onset PD (Cooper & Raamsdonk, 2018)	Mitochondrial kinase (Cooper & Raamsdonk, 2018)	Acts with Parkin in mitophagy (Cooper & Raamsdonk, 2018)	Increased stress sensitivity, reduction in basal slowing, mitochondrial accumulation, wild type dopamine neuron survival (Cooper & Raamsdonk, 2018)
lrk-1	LRRK2/PARK8 Autosomal dominant typical late-onset PD (Li, Tan, & Yu, 2014)	Large protein with kinase domain and ROC-GTPase domain (Li, Tan, & Yu, 2014)	Neurite outgrowth, cytoskeletal maintenance, vesicle trafficking, & autophagic protein degradation (Li, Tan, & Yu, 2014)	Decreased dopamine levels, deficits in dopamine-dependent behaviors (Cooper & Raamsdonk, 2018)
djr-1.1	DJ1/PARK7 Autosomal recessive early onset PD (Cooper & Raamsdonk, 2018)	Deglycase (Cooper & Raamsdonk, 2018)	Antioxidant, transcriptional regulation, molecular chaperone, protein degradation (Hijoka et al., 2017)	Increased sensitivity to oxidative stress, mitochondrial fragmentation, no loss of dopamine or dopamine-dependent behaviors (Cooper & Raamsdonk, 2018)
sodh-2	ADH4 Not a known PD gene	Dehydrogenase (Gao et al., 2018)	Unknown	α-syn aggregation (Knight et al., 2014)

The *unc-26* gene is the major focus of this study and warrants further discussion. *unc-26* is the ortholog to human *SYNJ1/PARK20*. This gene encodes a phosphoinositide phosphatase which is localized to synapses (Drouet & Lesage, 2014). SYNJ1 is crucial for autophagosomal and endosomal trafficking, synaptic vesicle recycling, and phosphoinositide metabolism (Ando et al., 2020). Missense mutations in *SYNJ1* are

associated with an autosomal recessive form of atypical early-onset PD (Drouet & Lesage, 2014). This type of PD is atypical in that these patients show a wide range of phenotypes, including seizures (Xie et al., 2019).

SYNJ1 is a 145 kDa protein with 3 domains (Drouet & Lesage, 2014). It contains a polyphosphoinositide phosphatase domain similar to the yeast Sac1 protein, a PI 5-phosphatase domain (5'PP), and a proline-rich domain (PRD) (Figure 2) (Todd et al., 2000). *SYNJ1*-related PD can occur from mutations in the Sac1 domain (Drouet & Lesage, 2014) or the 5'PP domain (Xie et al., 2019). In the e1196 *unc-26* mutant used in this study, there is an insertion mutation in the 5'PP domain (Todd et al., 2000).
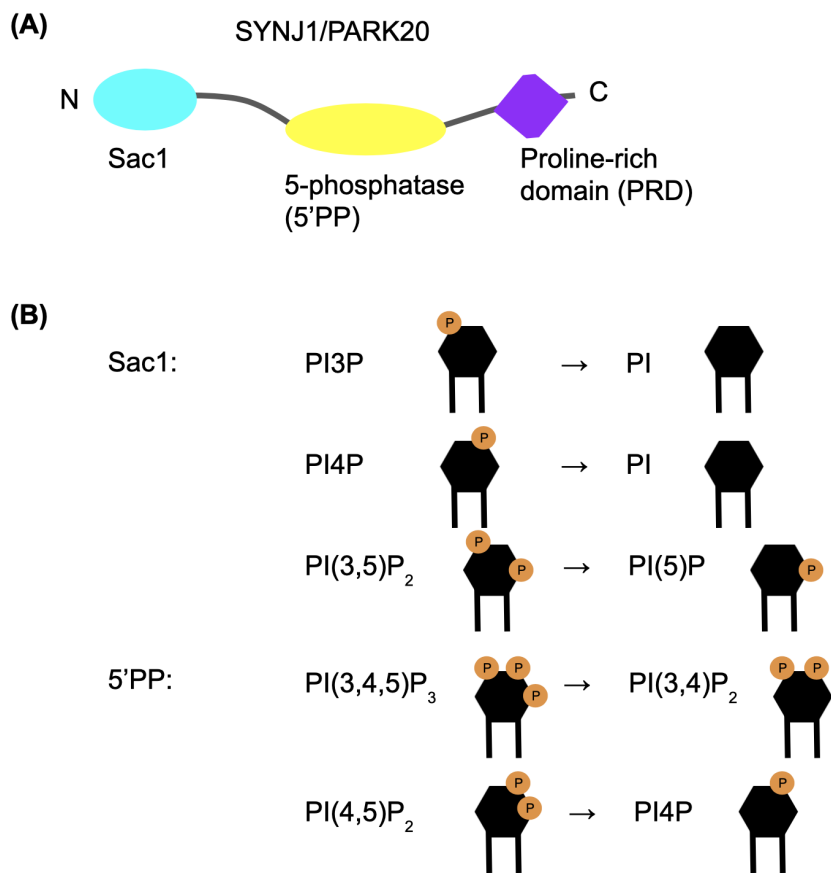
Figure 2. SYNJ1/PARK20 is a phosphoinositide phosphatase implicated in Parkinson's disease. (A) SYNJ1 contains an N-terminal Sac-1 like polyphosphoinositide phosphatase domain, a 5-phosphatase domain, and a C-terminal proline-rich domain. (B) SYNJ1 can cleave 3-, 4-, and 5- phosphates from phosphoinositides (Todd et al., 2000). Typically, it dephosphorylates bi- or triphosphates which are localized to plasma membranes, as well PI monophosphates in the membranes of the Golgi apparatus and endosomes (Fasano et al., 2018).

SYNJ1 has been shown to interact with endophilin, an endocytic protein involved in membrane bending, and the pair is rapidly recruited to clathrin coated pits during prolonged synaptic stimulation (Drouet & Lesage, 2014). Further studies have shown that the Sac1 domain is involved in targeting SYNJ1 to the synapse (Dong et al., 2015). The PRD is able to facilitate protein-protein interactions with synaptic vesicle components, which allows for efficient synaptic vesicle recycling (Drouet & Lesage, 2014). Since negative curvature is necessary for vesicle bud formation, SYNJ1 may help in creating membrane curvature by removing negative phosphate groups from the inner membrane surface (Todd et al., 2000). At endosomes, SYNJ1 is needed to dephosphorylate $PI(4,5)P_2$, which leads to the shedding of endocytic factors (Cao et al., 2017). In HeLA cells, loss of SYNJ1 has been shown to increase the number and size of early endosomes (Fasano et al., 2018). Overall, the implication of SYNJ1 in PD indicates that there is a link between synaptic vesicle recycling, endosomal trafficking, and PD.

This connection between synaptic vesicles and PD further connects lipids to PD, as synaptic vesicles have a unique lipid composition (Lewis et al., 2017). Lewis et al. found that synaptic vesicles are enriched in sphingolipids and triglycerides, which they suggest implicates these lipids in neurotransmitter release (2017). Further, they found that in the membrane of synaptosomes, which is a sample isolated from a synaptic terminal, there was an increase in PE, PG, and PS species (Lewis et al., 2017). These unique lipid landscapes in synaptic vesicles and synaptosomes suggest that impacts on lipid composition would increase one's probability of developing PD.

8. *B. subtilis*: A Potential Probiotic Treatment for Parkinson's Disease

Bacillus subtilis is a model beneficial bacterium (Donato et al., 2017). Recently, the formation of *B. subtilis* biofilms were demonstrated to increase *C. elegans* lifespan (Donato et al., 2017). *B. subtilis* was used as a treatment in a PD model of *C. elegans* (Goya et al., 2020). In this established *C. elegans* PD model, the nematodes overexpress human α-syn (Goya et al., 2020). The researchers were interested in studying the potential for probiotics to treat PD, since increasing evidence shows that signals from the gastrointestinal tract and the gut microbiota are involved in PD progression (Goya et al., 2020). By feeding *C. elegans* the *B. subtilis* strain PXN21, a strain which is viable for human consumption, the researchers were able to inhibit, delay, and reverse α-syn aggregation (Goya et al., 2020). They found that *B. subtilis'* benefits were mediated through changes in sphingolipid metabolism (Goya et al., 2020). This result, they

propose, could mean that *B. subtilis* alters the lipid composition of *C. elegans,* which directly influences α-syn aggregation (Goya et al., 2020). The lipid composition of *B. subtilis* has been probed by Bernat et al. (2016), specifically in the DSM 3257 and I'1a strains. LC-MS analysis demonstrated that PGs made up two-thirds of the total phospholipid fraction, and PEs were the second most abundant class, at 21-31% abundance (Bernat et al., 2016).

Materials & Methods

Worm Strains

N2 (WT)
RB2510 *capt-6 [W08D2.5(ok3473)]*
CB1196 *unc-26(e1196)*
RB2547 *pink-1(ok3538)*

Strains were provided by the Caenorhabditis Genetics Center (CGC), which receives funding from the NIH Office of Research Infrastructure Program (P40 OD010440). The *capt-6* and *pink-1* strains were provided to the CGC by the *C. elegans* Gene Knockout Project at the Oklahoma Medical Research Foundation, which was part of the International *C. elegans* Gene Knockout Consortium.

Bacterial Strains

E. coli (OP50)
B. subtilis (sp168)

B. subtilis (sp168) was provided by the Walhout lab at UMMS

The following HT115 bacteria transformed with RNAi were obtained from the Ahringer library:
L4440 (empty vector)
fat-7 (F10D2.9)
pink-1 (EEED8.9)
lrk-1 (T27C10.6)
djr-1.1 (B0432.2)
catp-6 (W08D2.5)
unc-26 (JC8.10)
sodh-2 (K12G11.4)

Nematode Growth Conditions

All strains were maintained on HG plates seeded with *E. coli* (OP50) and incubated at 20°C. Nematodes were synchronized for experiments by bleaching gravid adults and rotating the hatching eggs in M9 buffer for 20-24 hours at 20°C. Synchronized L1s were

grown at 20°C at a density of 2,000 animals per 10 cm NGM-CI plate or 5,000 animals per 10 cm HG plate. NGM-CI plates were prepared by adding 0.5 mL of carbenicillin (100 mg/mL) and 1 g of isopropyl β-D-thiogalactoside (IPTG) to 1L of Normal Growth Media. NGM-CI plates were seeded with *L4440* bacteria 48-72 hours in advance of use and stored at 20°C. HG plates were seeded with OP50 bacteria 24 hours before use and stored at room temperature.

Bacteria Cultures and Growth Conditions

To make *E. coli* or *B. subtilis* cultures, 6 mL of LB media was inoculated with 2-3 colonies and shaken overnight at 37°C. Resultant culture was stored at 4°C. To make RNAi bacteria cultures, LB media containing 100 μg/mL carbenicillin and 15 μg/mL tetracycline was inoculated and shaken overnight at 37°C. Resultant culture was stored at 4°C.

Adult-Only RNAi

Synchronized L1s were plated on *L4440* seeded NGM-CI plates and stored at 20°C. 48 hours after plating, young adult animals were collected in 1X M9 and washed 3 times. Young adult animals were then transferred to the RNAi seeded plates and stored at 20°C. 24 hours after transferring to RNAi, additional concentrated RNAi bacteria culture was added to each plate to prevent starvation. After an additional 24 hours, Day 3 adults were harvested and washed with M9. Adults were partially separated from larval animals by gravity separation (3 separations, about 2 minutes each). *C. elegans* samples were stored at -80°C.

Mutant Animal Phospholipid Characterization Timeline

48 hours after plating L1 mutant animals on *L4440* seeded NGM-CI plates, L1s had grown to young adults and were collected in M9 and washed 3 times. Young adult animals were then transferred to fresh *L4440* seeded plates and stored at 20°C. 48 hours later, Day 3 adults were harvested and washed with M9. Adults were partially separated from larval animals by gravity separation (3 separations, about 2 minutes each). *C. elegans* samples were stored at -80°C.

^{15}N Stable Isotope Labeling Strategy

Hatched L1s (N2s or *unc-26* mutants) were plated on OP50 seeded HG plates. 48 hours after plating, Day 1 animals were transferred to fresh OP50 seeded HG plates. 24 hours later, animals were again transferred to fresh plates. During this transfer, N2 adult animals were separated from larval animals by gravity separation (3 separations, about 2 minutes each). Next, the ^{15}N stable isotope labeling procedure described by Dancy et al. (2015) was followed with modifications. Briefly, OP50 colonies were separately cultured in ^{14}N-LB or ^{15}N-Isogro (Sigma Aldrich) media for 16-18 hours at 37°C, harvested, and then resuspended in M9 at a 0.15 g/mL. 10 cm agarose plates were seeded with 800 µL of a 1:1 mixture of ^{14}N:^{15}N or 800 µL of ^{14}N and dried. Immediately, N2 or *unc-26* Day 4 animals were transferred to the labeled or unlabeled plates. Animals were harvested after 24 hours and stored at -80°C.

Total Lipid Extraction

To extract total lipid fractions, first frozen worm samples (8,000 to 10,000 animals) were added to 4mL chloroform:methanol (2:1) solution (Dancy et al., 2015). 10 µL of internal lipid standards, (PC 11:0, TAG 13:0) were added to each sample, and the samples rotated at room temperature for 1.5 hours (Dancy et al., 2015). Samples were cleaned with 600 µL 0.9% NaCl, and centrifuged for 2 minutes at 735 x *g*. The fraction of the sample containing the total lipid extract was isolated and dried under nitrogen stream (Drechsler et al., 2016). Lipids were dissolved in 200 µL acetonitrile/2-propanol/water (65:30:5 v/v/v) dilution buffer (Drechsler et al., 2016).

HPLC-MS/MS Method and Data Analysis

10 µL of resuspended lipids were injected onto the HPLC-MS/MS, set to negative scanning mode (Dancy et al., 2015). The HPLC system used was a Dionex UHPLC UltiMate 3000, equipped with a C_{18} Hypersil Gold 2.1 x 50mm, 1.9µm column (25002-052130; Thermo Scientific) and a 2.1 mm ID, 5 µm Drop-In guard cartridge (25005–012101; Thermo Scientific). The HPLC was coupled with an Dionex UltiMate 3000 RS quaternary pump, a Dionex UltiMate 3000 RS autosampler, and a Q Exactive Orbitrap mass spectrometer from Thermo Scientific with a heated electrospray ionization (HESI) source.

Data analysis was performed using Lipid Data Analyzer (LDA) software (Version 2.8.0) (Hartler et al., 2011). LDA uses exact mass, retention time, and predicted isotope

distribution from full-profile, negative-ion-mode MS1 scans to distinguish lipids (Drechsler et al., 2016). In LDA, MS was set to 'OrbiTrap_Exactive' and Fragment Selection was set to 'noIntensity'. RAW files from the negative ion mode MS1 scans were analyzed using a 0.1% relative peak cut-off value. The RAW files were run against an LDA exact mass list for PC, PE, PS, PG, PI, P-PE, P-PC, O-PE, O-PC, LPC, LPE, and LPS (Olsen Lab).

For analysis of the relative abundance of each phospholipid type, lipid species containing less than 24 carbons and 0 double bonds or greater than 40 carbons and 10 doubles bonds were excluded, as the phospholipids present in *C. elegans* would generally be within this range (Watts & Ristow, 2017). Accordingly, lyso-lipids were excluded if they contained less than 12 carbons and 0 double bonds or greater than 20 carbons and 5 double bonds. Species whose relative abundance was less than 0.01% were also excluded. Relative abundance was recalculated after exclusions.

The same exclusions described above were used when determining phospholipid saturation. After exclusions, the number of lipids containing 0, 1, 2-3, 4-5, 6-7, or greater than 8 doubles bounds were counted and the relative distribution of each class was determined.

[15]N-isotope incorporation was calculated manually by measuring the isotope peak intensities in the Thermo Qual Browser Software in Xcalibur version 2.2 (Thermo Scientific). The percent of new phospholipid synthesis was calculated as previously reported by Dancy et al. (2015). Briefly, the unlabeled animal sample was utilized to determine natural isotope abundance, which was then subtracted from the ^{15}N-labeled animals to determine the incorporation of the exogenous [15]N.

Brood Size and Timing Assay

3cm NGM plates were seeded with OP50 or *B. subtilis* and grown at room temperature for at least 24 hours. 150 synchronized L1s were plated onto 3cm NGM plates seeded with OP50 or *B. subtilis* and stored at 20°C. 48 hours later, Day 1 animals were transferred to individual 3cm plates, with 5 to 7 plates per condition. For the next 17 days, the number of eggs and L1s on each plate were counted. Animals were transferred to fresh plates any day that there were eggs or L1s present, or at least every two days. Plates with eggs and L1s were retained for 24 hours at 20°C and recounted to assess viability.

Results & Discussion

RNAi Screening of Parkinson's Disease Genes in *C. elegans* to Identify Changes in Phospholipid Profiles

In order to understand the role of lipids in PD, we profiled the phospholipid composition of *C. elegans* PD models. First, RNAi was used to knockdown orthologs of known human PD genes in *C. elegans* to generate the disease models (see Table 1). Young adult animals were fed RNAi bacteria for 48 hours. The animals were collected and the total lipid content present in the animals were extracted and analyzed using HPLC-MS/MS. To validate that RNAi induction was effective, *fat-7* RNAi was used as a positive control. Work by Dancy et al. (2015) has previously shown that there are significant alterations in PC and PE composition following *fat-7* knockdown, and we replicated this (Figure 3B). One discrepancy was that a significant decrease in PC 38:6 was found here that was not observed by Dancy et al.

In analyzing the obtained mass spectrometry data, we first took a global approach, analyzing the overall relative distribution of 12 major phospholipid classes: PCs, PIs, P-PCs, P-PEs, O-PCs, O-PEs, PIs, PSs, PGs, LPCs, LPEs, and LPSs (Figure 3A). PCs, PEs, PIs, and PSs are all critical structural components of eukaryotic membranes (van Meer, Voelker, & Feigenson, 2008). The P-PC, P-PE, O-PC, and O-PE lipid species differ from the PC and PE classes in that they contain ether linkages rather than acyl linkages. Ether linkages change the biophysical properties of the lipid, making lipid domains containing these species less fluid than those containing acyl-linked phospholipids (Drechsler et al., 2016). Ether lipids may also function in cell signaling and antioxidant scavenging (Drechsler et al., 2016). Lyso phospholipids, including LPCs, LPEs, and LPSs, function in cell signaling as messenger lipids (van Meer, Voelker, & Feigenson, 2008).

Analysis of the animals fed *pink-1, unc-26, catp-6, lrk-1, djr-1.1,* or *sodh-2* RNAi bacteria revealed no significant difference compared to the *L4440* control in overall phospholipid composition (Figure 3A) or in the abundance of individual PC and PE species (Figure 3B). However, there were trends towards increased PC abundance in the *unc-26* and *catp-6* knockdown animals (Figure 3A). This result suggests that phospholipid composition may be altered in these animals and thus we concluded that *unc-26* and *catp-6* should be further studied in regard to their relationship to phospholipids.

We speculate that PD RNAi did not have effects for several reasons. First, the timing and the limited duration of RNAi bacteria feeding, which was initiated at the beginning of adulthood and only done for 48 hours, could have been a significant factor. We chose to start RNAi during adulthood in order to model PD more accurately, because PD typically manifests in older populations. However, the genes chosen could be more critical during development compared to adulthood, leading to no observable changes during adult-only RNAi. Also, neurons may not have been particularly sensitive to RNAi, as has previously been reported (Cooper & Raamsdonk, 2018). This lack of knockdown in neurons would mean there was not a strong PD phenotype, as dopamine signaling should ultimately be altered when modeling PD. Finally, there is the potential that deficiencies in these genes simply do not change the phospholipidome.
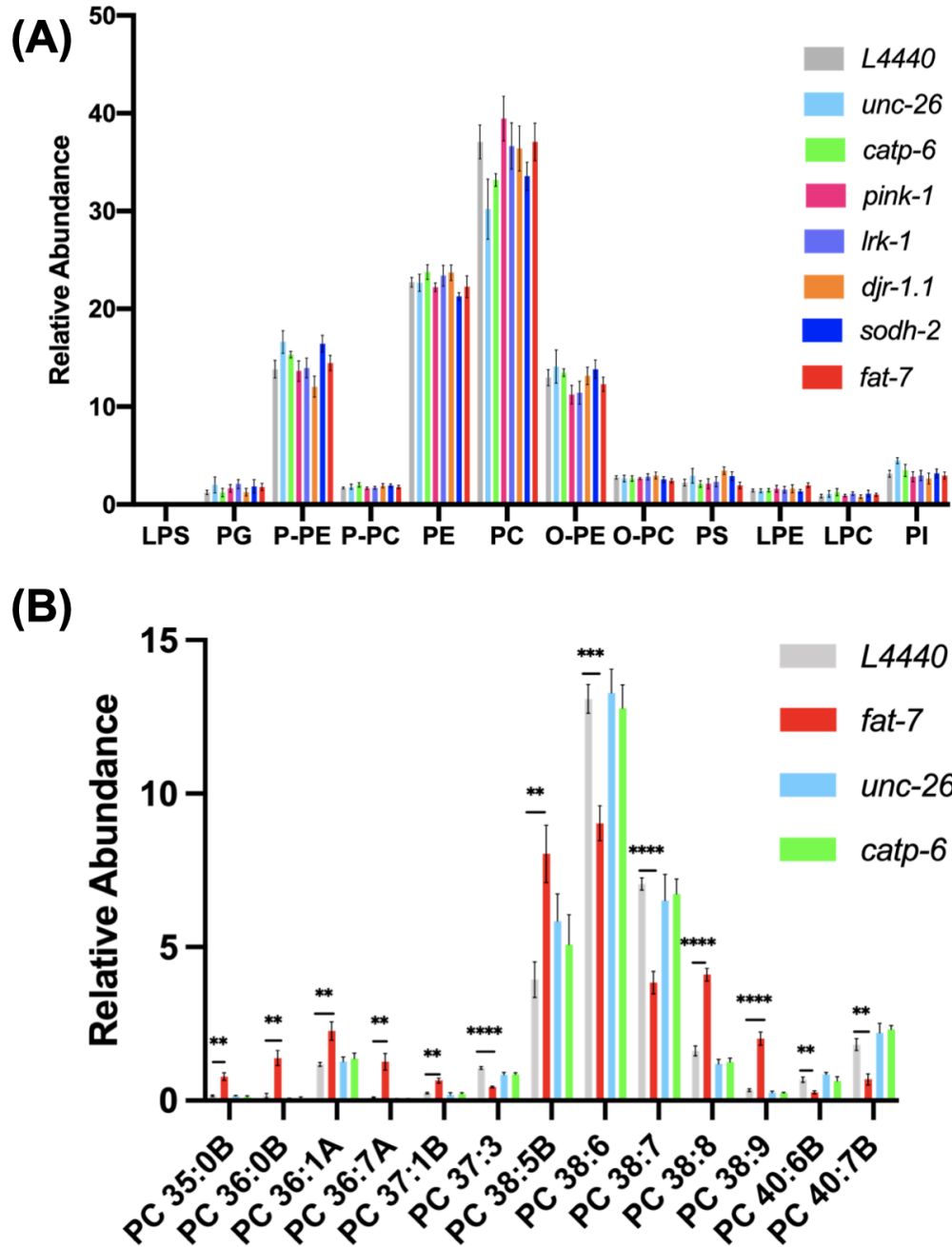
Figure 3. The phospholipid profiles of N2s following adult-only RNAi knockdown of PD related genes are consistent with the control. (A) Overall phospholipid distribution following adult-only RNAi. See text for a description of the lipid classes listed. Control animals were fed *L4440* (empty vector) bacteria. (B) Relative abundance of PC species in control animals versus animals fed *fat-7, unc-26, or catp-6* RNAi. PC lipids are written with the X:Y nomenclature, where X is the number of carbons in FA tails and Y indicates the total number of double bonds. If a single PC species had multiple retention times (with a greater than 0.75 minute difference in retention), the species

were denoted 'A' and 'B' to distinguish them. Only PC species with significant differences are shown. Numbers shown represent the mean of at least 4 biological replicates. Error bars represent $\pm$SEM. Unpaired t-tests were performed with GraphPad Prism 9. Significant changes as are indicated by * ($p<0.05$), ** ($p<0.01$), *** ($p<0.001$), and **** ($p<0.0001$).

unc-26 Mutants Have Altered Overall Phospholipid Composition

Given the trends towards decreased PC abundance after RNAi knockdown of *unc-26* and *catp-6* (Figure 3A), we followed up by profiling the phospholipid compositions of mutant *unc-26(e1196)* and *catp-6(ok3473)* animals. By studying mutant animals, we could see how lipid composition was affected when these proteins were non-functional throughout development and adulthood. This analysis demonstrated the same trend of decreased PCs in *unc-26* mutants, but not in *catp-6* mutants (Figure 4). Additionally, *unc-26* mutants show significantly increased PE lipids, and significantly decreased O-PC and LPC lipids. This change in phospholipid composition indicates that membranes are altered in *unc-26* mutants. Specifically, we suggest that membrane curvature is affected in this mutant, as PEs are important structural components in membranes, helping to promote the negative curvature necessary for membrane budding, fusion, and fission (van Meer, Voelker, & Feigenson, 2008).

This finding is complemented by the fact that *unc-26* (ortholog to human *SYNJ1/PARK20*) encodes a phosphoinositide phosphatase, which is critical for synaptic vesicle recycling, autophagosomal/endosomal trafficking, and phosphoinositide metabolism (Ando et al., 2020). Todd et al., have suggested that SYNJ1 may help in creating membrane curvature by removing negative phosphate groups from the inner membrane surface, helping to promote the curvature necessary for vesicle bud formation (2000). More insights into SYNJ1 function were gained from a study in HeLa cells, in which loss of SYNJ1 resulted in an increase in the number and size of early endosomes (Fasano et al., 2018). Thus, the increased PE abundance observed in *unc-26* mutants (Figure 3A) could indicate that cells are compensating for deficiencies in synaptic vesicle recycling or endosomal trafficking by modulating membrane curvature. Alternatively, these changes could be pathological, and potentially the result of a build up of endosomes.
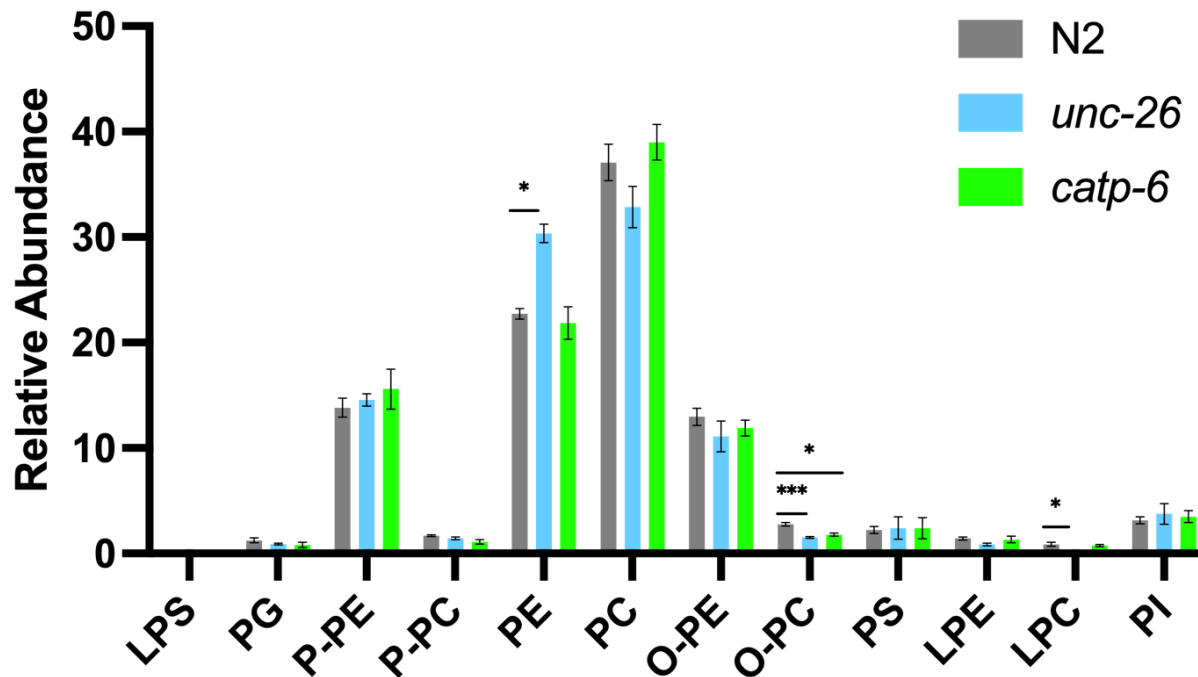
Figure 4. Phospholipid profiles of wild type (N2) animals compared to PD mutants show altered phospholipid composition in the *unc-26* mutant. Animals were collected 96 hours after hatching. Subsequent lipid extraction and HPLC-MS/MS was used to detect phospholipid abundance. n=5. Error bars represent $\pm$SEM. Unpaired t-tests were performed with GraphPad Prism 9. Significant changes as are indicated by * (p<0.05), ** (p<0.01), and *** (p<0.001).

To further characterize the lipid composition of *unc-26* mutants, we probed the differences between individual PE, PC, and PI lipids (Figure 5). This analysis revealed no significant changes between *unc-26* mutants and wild type animals. However, there are some trends: decreased PE 37:5, PI 35:0, and PI 36:0, and increased PI 38:5. A decrease in PI corroborates the activity of UNC-26 in converting PIP species to PIs. More replicates would be needed to verify these trends.
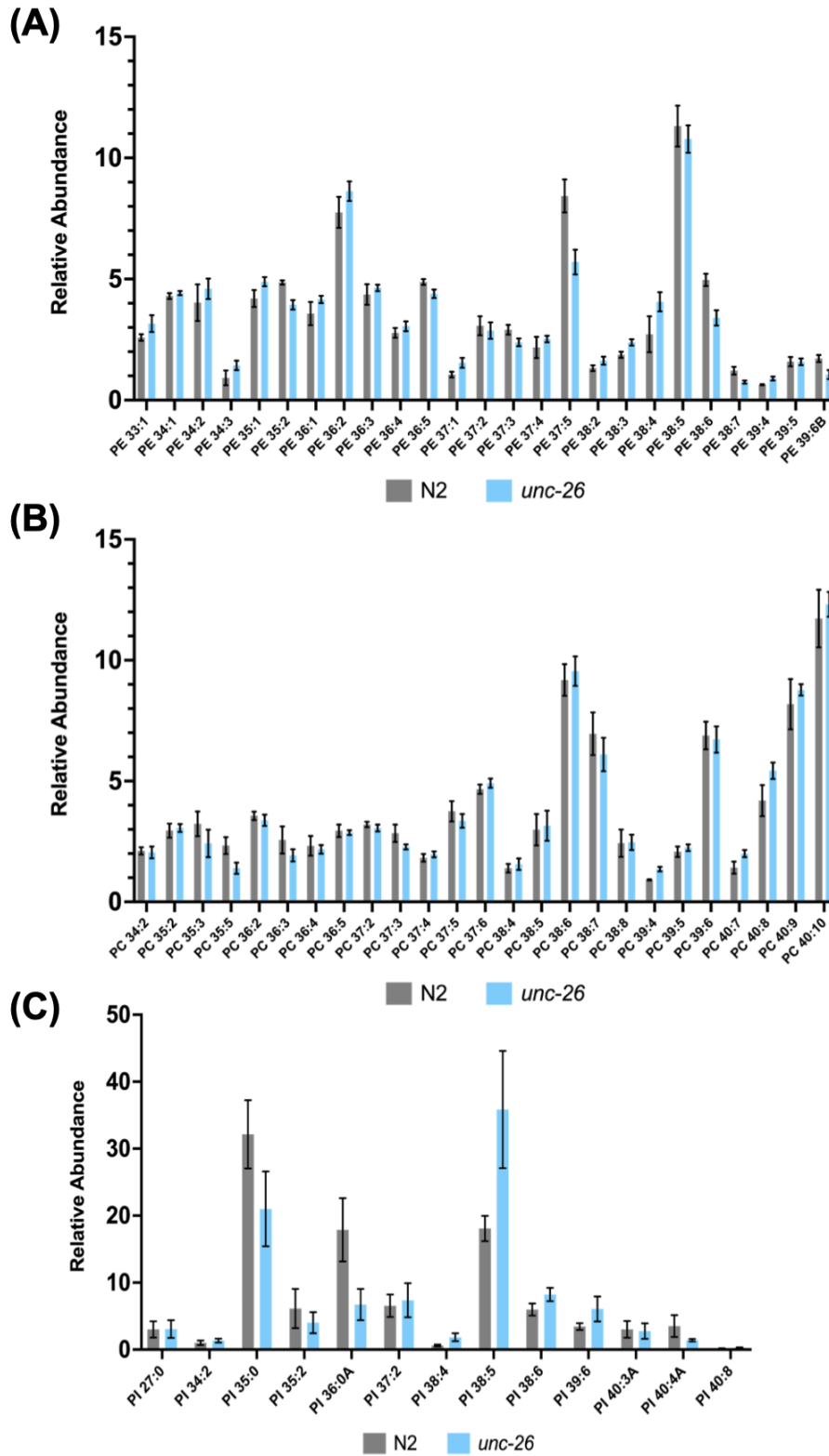
Figure 5. PE, PC, and PI lipid species relative abundance remain consistent between wild type (N2) animals and *unc-26* mutants. Animals were collected 120 hours after

hatching. Subsequent lipid extraction and HPLC-MS/MS was used to detect phospholipid abundance. Lipids are written with the X:Y nomenclature, where X is the number of carbons in FA tails and Y indicates the total number of double bonds. If a single species had multiple retention times (with a greater than 0.75 minute difference in retention), the species were denoted 'A' and 'B' to distinguish them. (A) The 25 most abundant PE lipids detected. (B) The 25 most abundant PC lipids detected. (C) The 13 most abundant PI lipids detected. n=4. Error bars represent ±SEM. Unpaired t-tests were performed with GraphPad Prism 9.

Phospholipid Saturation in *unc-26* Mutants is Similar to Wild Type Animals

Saturation of fatty acids within phospholipids is a key determinant of membrane fluidity, with decreased saturation leading to more fluidity. To determine if phospholipid saturation changes in the *unc-26* mutant, we binned the phospholipids detected above by the number of double bonds present in intact phospholipids. This analysis exhibited that phospholipid saturation remains consistent between *unc-26* and wild type animals (Figure 6). In healthy animals, membrane fluidity is regulated to maintain proper membrane function (Sultana & Olsen, 2020). Further, saturation can impact membrane trafficking (Vanni et al., 2019). Specifically, some proteins sense the ratio of saturated to unsaturated lipids (Vanni et al., 2019). The lack of change in membrane saturation shown suggests that in the *unc-26* model of PD, membrane fluidity is not majorly disrupted, and does not contribute to PD pathology.
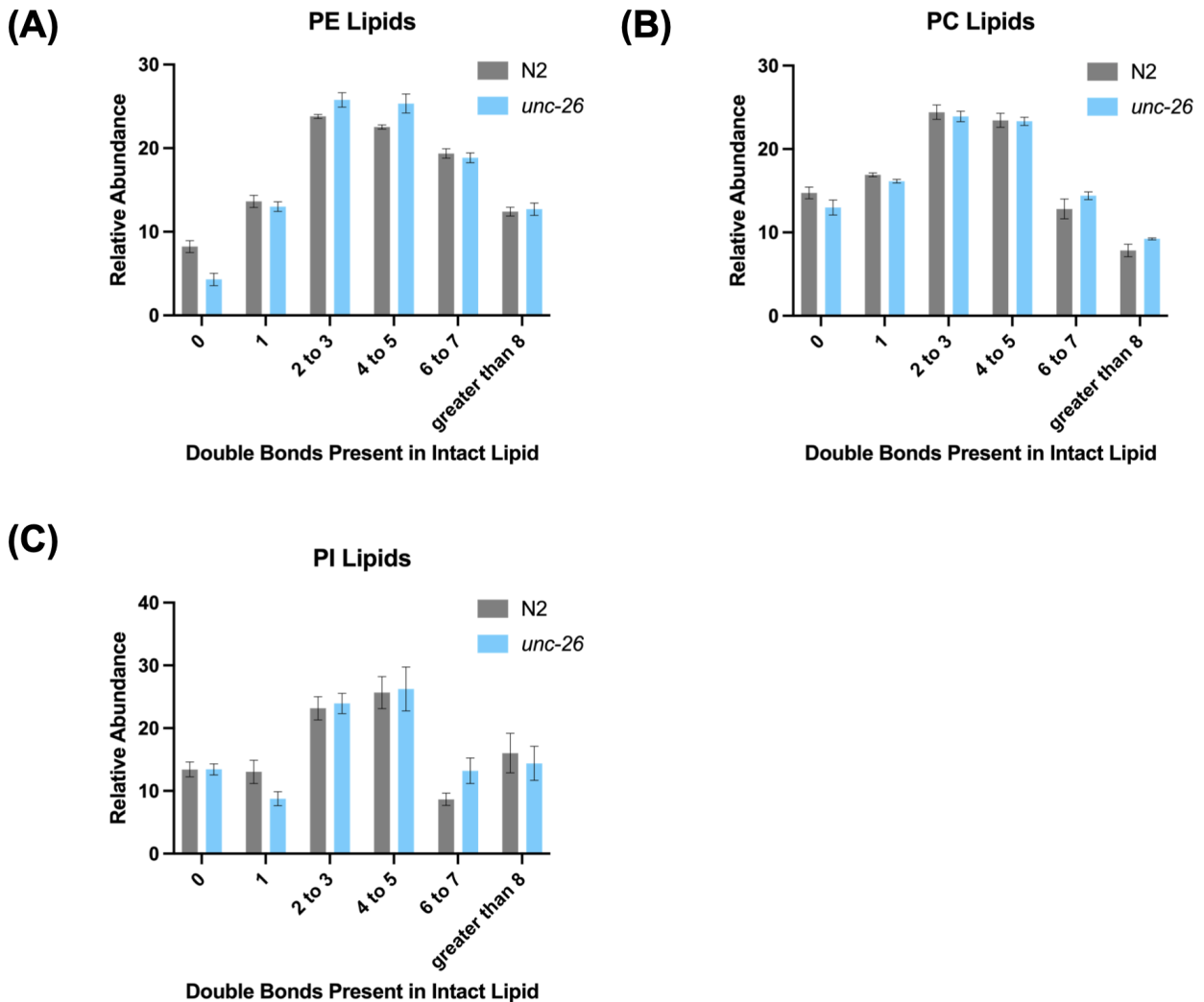
(A) PE Lipids

(B) PC Lipids

(C) PI Lipids

Figure 6. PE, PC, and PI lipid saturation remains consistent between wild type (N2) animals and *unc-26* mutants. Animals were collected 120 hours after hatching. Subsequent lipid extraction and HPLC-MS/MS was used to detect phospholipid abundance. Lipids were binned based on the number of double bonds present, and the relative distribution of each bin was calculated. (A) PE lipid saturation. (B) PC lipid saturation. (C) PI lipids saturation. n=4. Error bars represent $\pm$SEM. Unpaired t-tests were performed with GraphPad Prism 9.

^{15}N Labeling Reveals That *unc-26* Animals Trend Towards Decreased Phospholipid Turnover

We sought to better understand the mechanism by which phospholipid composition becomes altered in *unc-26* mutants by studying phospholipid turnover. By feeding the nematodes a diet enriched in the stable isotope ^{15}N for 24 hours, we were able to determine the percent ^{15}N incorporation in individual phospholipid species, which indicates the amount of turnover taking place for these lipids (Figure 7A). The ^{15}N will incorporate only into the lipids that are synthesized during the labeling period, which will allow for the analysis of membrane dynamics at the time of collection and avoid dilution effects.

This analysis showed that *unc-26* mutants exhibited a trend towards decreased phospholipid turnover for several PE and PC species (Figure 7B). An overall decrease in turnover may indicate reduced feeding of the animals; however, some lipids have a greater degree of decreased turnover, namely PC 39:6, PC 40:8, PC 40:9, and PC 40:10. Further replicates are required to fully define the dynamics of *unc-26* phospholipid turnover, but this initial result suggests that cells deficient in UNC-26 redistribute their PC and PE lipids, potentially to compensate for changes in synaptic vesicle recycling and endosomal trafficking in these mutants.
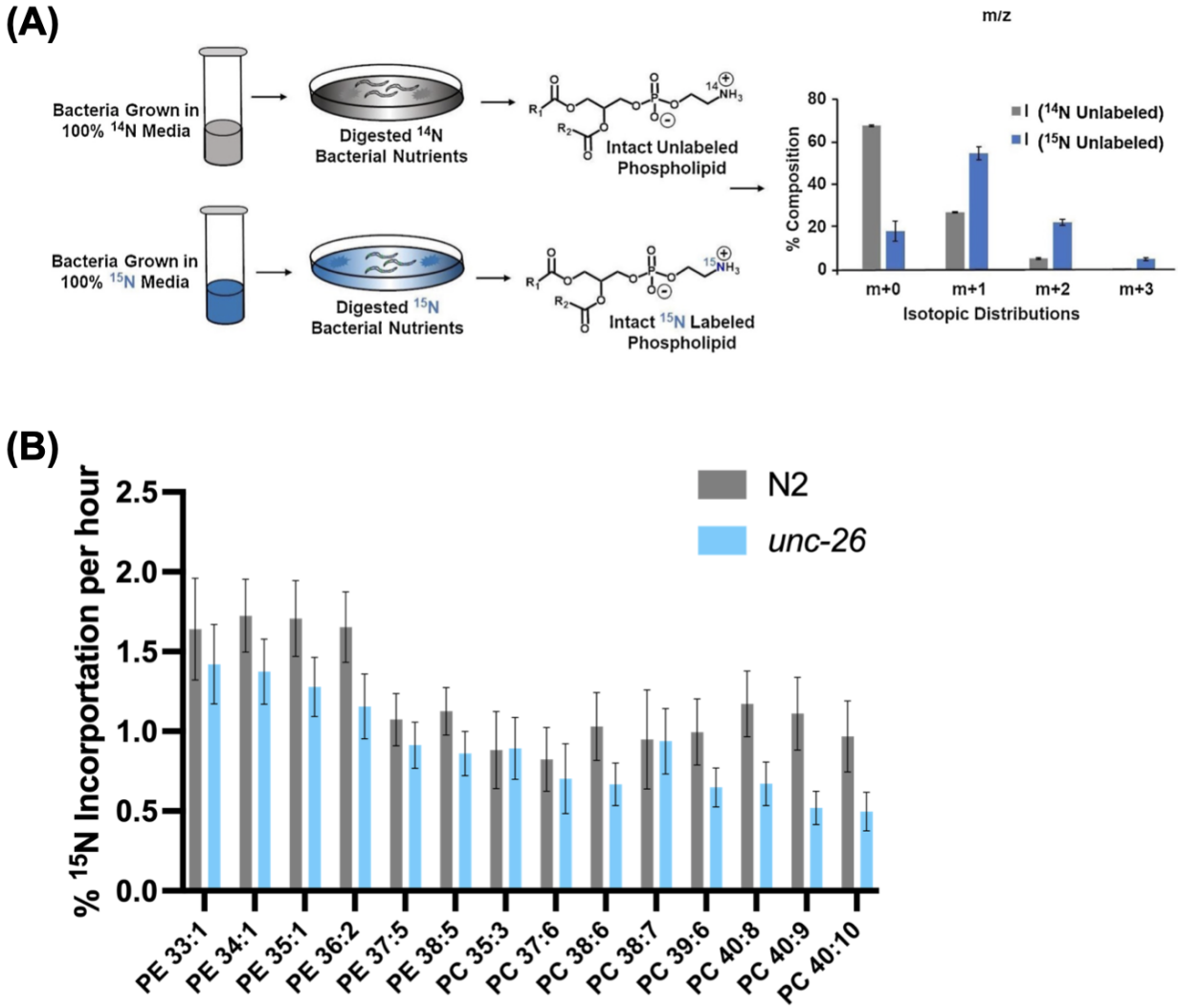
Figure 7. PE and PC lipids trend towards decreased turnover in *unc-26* mutants compared to wild type. (A) ^{15}N labeling strategy figure from Sultana & Olsen (2020). Briefly, intact phospholipid turnover can be assessed by feeding Day 3 adult *C. elegans* a ^{15}N labeled or ^{14}N unlabeled bacterial diet for 24 hours. In our study labeled plates were seeded with a 1:1 mixture of ^{15}N and ^{14}N bacteria. Depicted above is an example of ^{15}N incorporated into an ethanolamine head group. The resultant mass spectra isotopic distribution exhibits a reduction of the m+0 peak as well as increases in the m+1, m+2 and m+3 peaks in ^{15}N labeled lipid compared to unlabeled, which represents lipid turnover. (B) ^{15}N incorporation per hour of major PC and PE lipids in wild type (N2) animals or *unc-26* mutants. n=3. Error bars represent $\pm$SEM. Unpaired t-tests were performed with GraphPad Prism 9.

Dietary Intervention with *B. Subtilis* Modifies Phenotypes Observed in *unc-26* Mutants

The *unc-26* mutant is known to display altered movement phenotypes, including backwards movement with jerky motion and frequent coiling (Figure 8C) (Todd et al, 2000). Here we quantify another phenotype: altered fecundity. Not only is fecundity known to be controlled by dopamine in *C. elegans* (Maulik et al., 2017), but also fecundity has been shown to influence human PD outcomes (Frentzel et al., 2017). In female PD patients, the number of children, older age of menarche, and older age of menopause were shown to positively correlate with a delay of disease onset by up to 30 months (Frentzel et al., 2017). The mechanisms of how reproduction relates to PD are still unknown, and thus fecundity is an important assessment in PD models. In addition, fecundity is an ideal phenotype for identifying rescues, because it is easy to access.

To investigate fecundity, we isolated synchronized Day 1 nematodes on agar plates. The number of progeny produced each day by each worm was counted until reproduction ceased. This study demonstrated that *unc-26* mutants have delayed development, as on Day 3 of adulthood, N2s produced 47.0367±3.9648 percent of their brood, whereas *unc-26* mutants produced only 11.3267±10.6863 percent (p=0.0056, unpaired t-test) (Figure 8A). Also, *unc-26* reproduction continued for one week after N2 reproduction had ceased. Further, *unc-26* mutants have a significantly smaller brood size than N2s, with the *unc-26* brood size being 123±24.3 progeny, and N2s being 269±57.7 (Figure 8B).

With altered fecundity established, we sought to rescue this phenotype by dietary alteration. The probiotic bacterium *B. subtilis* has previously been shown to clear α-syn aggregates in a *C. elegans* strain overexpressing α-syn, but has not been assessed in other PD models (Goya et al., 2020). We first determined the phospholipid profile of *B. subtilis* compared to the standard *E. coli* (OP50) diet by HPLC-MS/MS (Figure 9). Although only one replicate was analyzed, our results are consistent with previous reports that *B. subtilis* contains about 66% PG species and 21-31% PE species (Bernat et al., 2016). The observed decrease in PE species in *B. subtilis* compared to OP50 (Figure 9) is relevant, as above we found that *unc-26* mutants have a significantly increased relative abundance of PEs (Figure 4). Accordingly, we hypothesized that by providing less PE to *unc-26*, the nematodes' conditions may be alleviated if increased PE abundance is a pathological aspect of its phenotypes.

Feeding *B. subtilis* to *unc-26* mutants, a further delay in reproductive timing was observed (Figure 8A). Interestingly however, the total brood size of *unc-26* mutants fed *B. subtilis* was significantly higher than those fed OP50 (Figure 8B). These results indicate that *B. subtilis* does have some effect on PD models deficient in UNC-26. We hypothesize that the thicker lawn grown by *B. subtilis* compared to OP50 may have impaired *unc-26* in its early development stage, leading to the delayed brood production shown. Further study of *B. subtilis*, including how it affects the phospholipid and fatty acid profiles of *unc-26* mutants, is warranted to understand the molecular mechanisms of the changes observed.
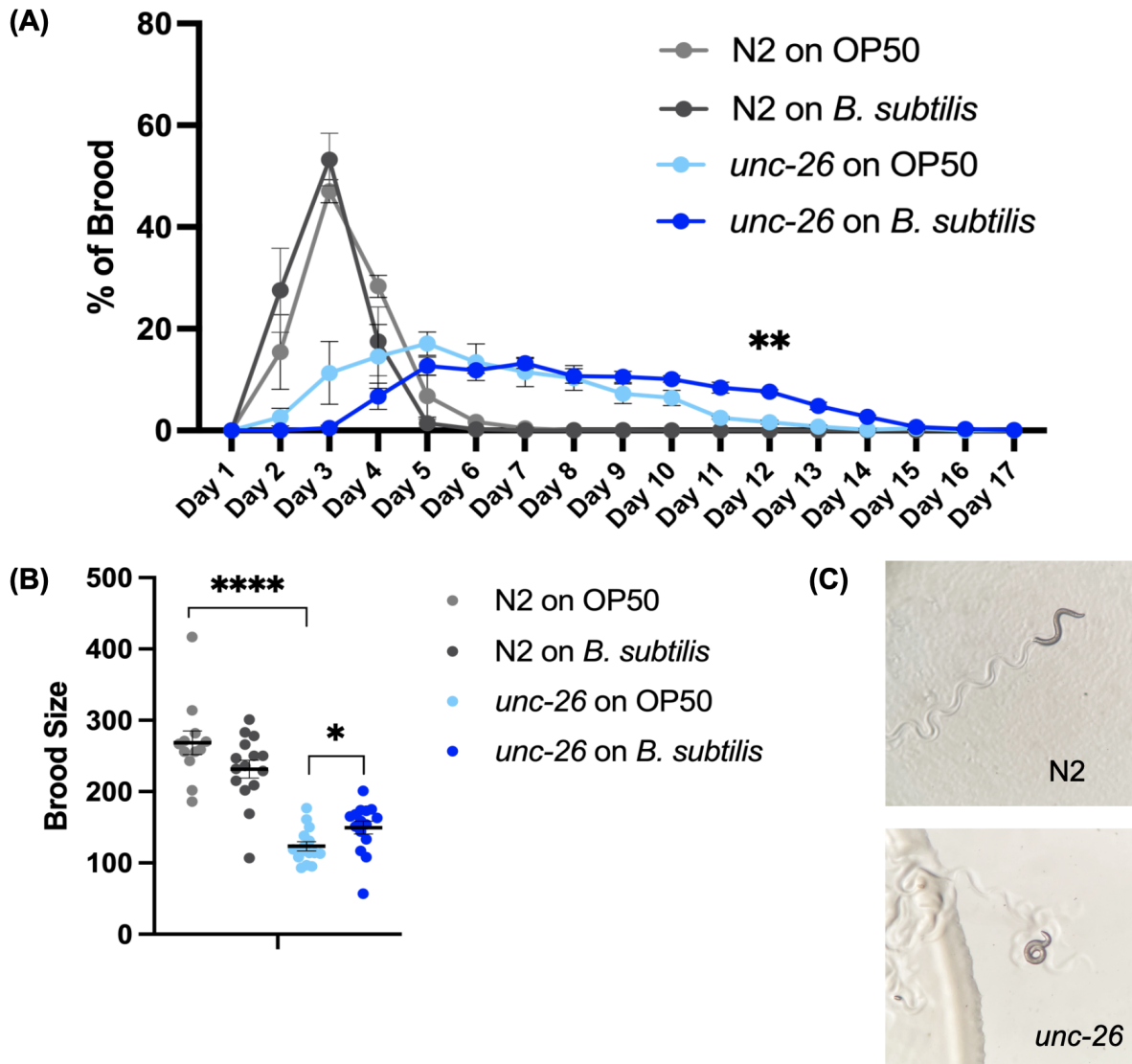
Figure 8. A *B. subtilis* diet changes the timing of brood production and brood size in *unc-26* mutants. (A) Assay characterizing timing of brood production in N2 and *unc-26* animals when fed an OP50 or *B. subtilis* diet. The y-axis represents the number of progeny produced each day divided by total progeny. Data shown is the mean of 3 biological replicates. Significance between the two *unc-26* groups is shown. (B) Total brood size of N2 or *unc-26* animals when fed an OP50 or *B. subtilis* diet. Each dot represents the brood from one individual (N2 on OP50: n=12, N2 on *B. subtilis*: N=15, *unc-26* on OP50: n=15, *unc-26* on *B. subtilis*: n=15). (C) Day 4 adult nematodes highlighting altered movement observed in *unc-26* mutants. Error bars represent $\pm$SEM. Unpaired t-tests with Welch correction were performed with GraphPad Prism 9. Significant changes as are indicated by * ($p<0.05$), ** ($p<0.01$), and **** ($p<0.0001$).
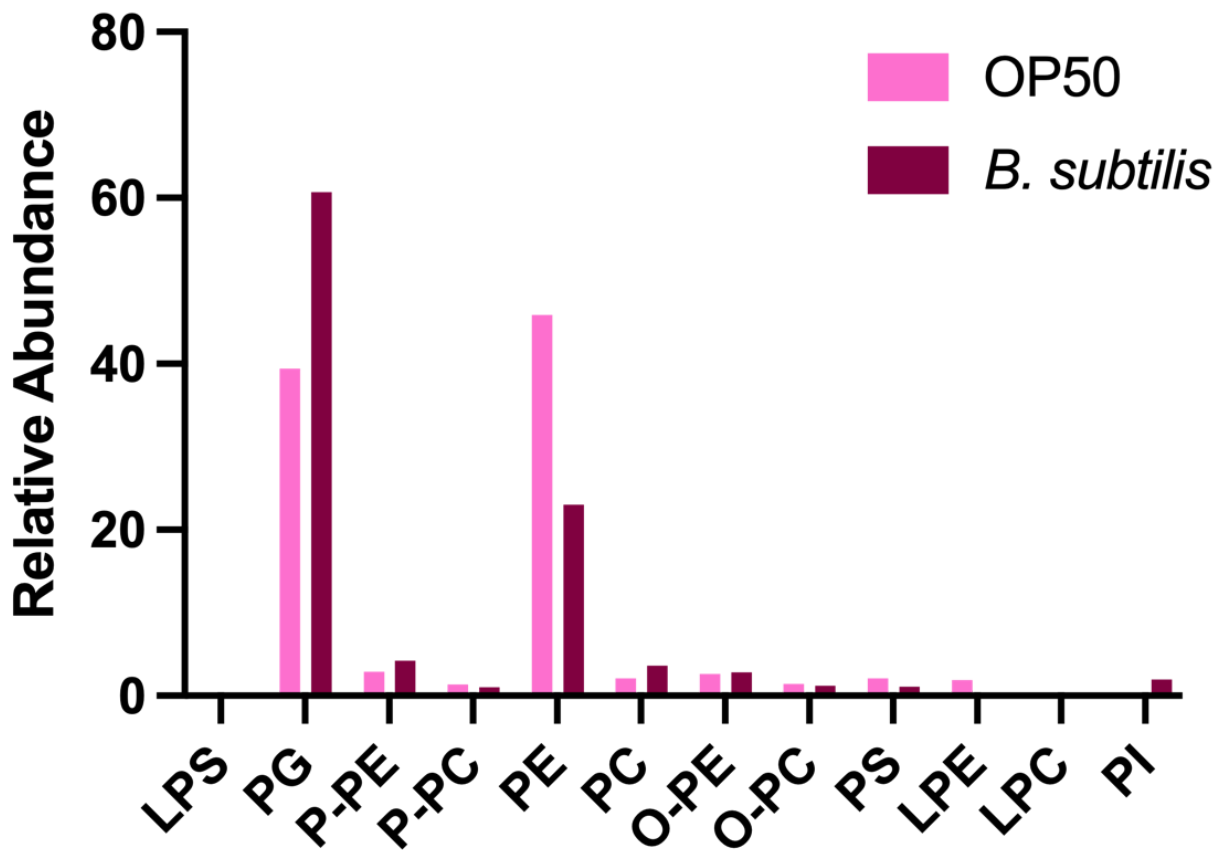
Figure 9. *E. coli* (OP50) and *B. subtilis* (sp168) phospholipid profiles. 100 μL of OP50 or *B. subtilis* culture were seeded onto HG plates and grown overnight at room temperature. Phospholipid profiles were obtained by lipid extraction, HPLC-MS/MS, and data analysis with LDA. n=1

Conclusions & Future Directions

In this study, a screen identified trends towards altered phospholipid composition in *C. elegan* models of PD after RNAi knockdown of *unc-26* or *catp-6*. Subsequent phospholipid analysis of *unc-26*(e1196) mutants revealed an increase of overall PE species abundance. Phospholipid dynamics in *unc-26* mutants were then characterized by stable isotope labeling and mass spectrometry. These initial studies show that there is differential downregulation of PC and PE lipids in this PD model. *unc-26* mutants are known to display several PD phenotypes, including altered movement. We also describe that *unc-26* has delayed development and decreased fecundity, which can be modified by dietary intervention with *B. subtilis*.

Future work is required to fully understand the mechanisms through which mutations in SYNJ1 lead to PD, and how *B. subtilis* can intervene. We hypothesize that there could be build up of early endosomes occurring in *unc-26* mutants, as has been shown in SYNJ1-deficient HeLa cells (Fasano et al., 2018). Alternatively, the increased PE abundance observed in *unc-26* could be a mechanism to rescue synaptic vesicle recycling. Specifically, loss of UNC-26 would lead to loss of proper synaptic vesicle membrane curvature (Todd et al., 2000), and PE compensation could assist in inducing membrane curvature, as PEs are prone to curving due to the geometry of the molecule.

To further define how membrane lipids are impacted by mutated *unc-26*, other *unc-26* strains should be subjected to HPLC-MS/MS analysis. The strain used here, e1196, contains an insertion in the 5'PP domain (Todd et al., 2000). Mutations within the Sac1 domain might have different phospholipid impacts, as this domain acts on different substrates than the 5'PP domain (Figure 2). Also of interest is how the phospholipid profile changes over time in PD models. This analysis could provide insights into how phospholipids could be used as a biomarker for PD and how membrane curvature impacts PD. Experiments probing *unc-26* phospholipids at different time points would be beneficial in this regard. Finally, studies of the phospholipidome of *unc-26* mutants fed *B. subtilis* could provide clues as to how *B. subtilis* affects these animals.

Overall, this study represents an early step towards the ultimate goal of establishing a diagnostic biomarker for PD. Evidently lipids change in PD, but the identification of a consistent and detectable change requires further research. Further, this study helps to define *PARK20*-related PD specifically, which will be useful when developing a precision medicine approach for treating *PARK20* patients. One potential treatment

could include dietary supplementation of certain lipids to help promote proper lipid composition. PD currently affects 1% of the human population above 60 years old (Xicoy, Wieringa, & Martens, 2019), and as the aging population increases, the need for a diagnostic or treatment for PD increases along with it.

Abbreviations

α-syn: α-synuclein
AD: Alzheimer's disease
B. subtilis: Bacillus subtilis
C. elegans: Caenorhabditis elegans
dsRNA: double-stranded RNA
FA: fatty acid
HG: High Growth Media
HPLC-MS/MS: High performance liquid chromatography tandem mass spectrometry
LB: Lysogeny broth
LC-MS: Liquid chromatography tandem mass spectrometry
LDA: Lipid Data Analyzer
LPC: Lysophosphatidylcholine
LPE: Lysophosphatidylethanolamine
LPS: Lysophosphatidylserine
NGM: Normal Growth Media
NGM-CI: NGM+ Carbenicillin and isopropyl β-D-thiogalactoside (IPTG)
O-PC: Plasmanylcholine
O-PE: Plasmanylethanolamine
PA: Phosphatidic acid
PC: Phosphatidylcholine
PD: Parkinson's disease
PE: Phosphatidylethanolamine
PI: Phosphatidylinositol
PIP: Phosphoinositide containing one phosphate group
PG: Phosphatidylglycerol
P-PC: Plasmenylcholine
P-PE: Plasmenylethanolamine
PRD: Proline-rich domain
PS: Phosphatidylserine
RNAi: RNA interference
Sac1: Sac1-like polyphosphoinositide phosphatase domain
TAG: Triacylglycerol
UMMS: University of Massachusetts Medical School
5'PP: 5-phosphatase domain

References

Anand N, Holcom A, Broussalian M, Schmidt M, Chinta SJ, Lithgow GJ, Andersen JK, Chamoli M. Dysregulated iron metabolism in C. elegans catp-6/ATP13A2 mutant impairs mitochondrial function. Neurobiol Dis. 2020 Jun;139:104786. doi: 10.1016/j.nbd.2020.104786. Epub 2020 Feb 5. PMID: 32032734; PMCID: PMC7150649.

Ando, K., Ndjim, M., Turbant, S. et al. The lipid phosphatase Synaptojanin 1 undergoes a significant alteration in expression and solubility and is associated with brain lesions in Alzheimer's disease. acta neuropathol commun 8, 79 (2020). https://doi.org/10.1186/s40478-020-00954-1

Bernat, P., Paraszkiewicz, K., Siewiera, P., Moryl, M., Płaza, G., & Chojniak, J. (2016). Lipid composition in a strain of Bacillus subtilis, a producer of iturin A lipopeptides that are active against uropathogenic bacteria. World journal of microbiology & biotechnology, 32(10), 157. https://doi.org/10.1007/s11274-016-2126-0

Cajka, T., & Fiehn, O. (2014). Comprehensive analysis of lipids in biological systems by liquid chromatography-mass spectrometry. Trends in analytical chemistry : TRAC, 61, 192–206. https://doi.org/10.1016/j.trac.2014.04.017

Cao M, Wu Y, Ashrafi G, McCartney AJ, Wheeler H, Bushong EA, Boassa D, Ellisman MH, Ryan TA, De Camilli P. Parkinson Sac Domain Mutation in Synaptojanin 1 Impairs Clathrin Uncoating at Synapses and Triggers Dystrophic Changes in Dopaminergic Axons. Neuron. 2017 Feb 22;93(4):882-896.e5. doi: 10.1016/j.neuron.2017.01.019. PMID: 28231468; PMCID: PMC5340420.

Cooper, J. F., & Van Raamsdonk, J. M. (2018). Modeling Parkinson's Disease in C. elegans. Journal of Parkinson's disease, 8(1), 17–32. https://doi.org/10.3233/JPD-171258

Dancy BC, Chen SW, Drechsler R, Gafken PR, Olsen CP. 13C- and 15N-Labeling Strategies Combined with Mass Spectrometry Comprehensively Quantify Phospholipid Dynamics in C. elegans. PLoS One. 2015;10(11):e0141850. Epub 2015/11/04. PubMed Central PMCID: PMCPmc4631354. Pmid:26528916

Donato, V., Ayala, F., Cogliati, S. et al. Bacillus subtilis biofilm extends Caenorhabditis elegans longevity through downregulation of the insulin-like signalling pathway. Nat Commun 8, 14332 (2017). https://doi.org/10.1038/ncomms14332

Drechsler R, Chen SW, Dancy BCR, Mehrabkhani L, Olsen CP (2016) HPLC-Based Mass Spectrometry Characterizes the Phospholipid Alterations in Ether-Linked Lipid Deficiency Models Following Oxidative Stress. PLOS ONE 11(11): e0167229. https://doi.org/10.1371/journal.pone.0167229

Drouet, V., & Lesage, S. (2014). Synaptojanin 1 mutation in Parkinson's disease brings further insight into the neuropathological mechanisms. BioMed research international, 2014, 289728. https://doi.org/10.1155/2014/289728

Dong, Y., Gou, Y., Li, Y., Liu, Y., & Bai, J. (2015). Synaptojanin cooperates in vivo with endophilin through an unexpected mechanism. eLife, 4, e05660. https://doi.org/10.7554/eLife.05660

Fanning, S., Selkoe, D. & Dettmer, U. Parkinson's disease: proteinopathy or lipidopathy?. npj Parkinsons Dis. 6, 3 (2020). https://doi.org/10.1038/s41531-019-0103-7

Farmer, K., Smith, C., Hayley, S., & Smith, J. (2015). Major Alterations of Phosphatidylcholine and Lysophosphotidylcholine Lipids in the Substantia Nigra Using an Early Stage Model of Parkinson's Disease. International Journal of Molecular Sciences, 16(8), 18865–18877. doi:10.3390/ijms160818865

Fasano, D., Parisi, S., Pierantoni, G.M. et al. Alteration of endosomal trafficking is associated with early-onset parkinsonism caused by SYNJ1 mutations. Cell Death Dis 9, 385 (2018). https://doi.org/10.1038/s41419-018-0410-7

Frentzel, D., Judanin, G., Borozdina, O., Klucken, J., Winkler, J., & Schlachetzki, J. (2017). Increase of Reproductive Life Span Delays Age of Onset of Parkinson's Disease. Frontiers in neurology, 8, 397. https://doi.org/10.3389/fneur.2017.00397

Gao AW, Smith RL, van Weeghel M, Kamble R, Janssens GE, Houtkooper RH. (2018). Identification of key pathways and metabolic fingerprints of longevity in C. elegans. Exp Gerontol. Nov;113:128-140. doi: 10.1016/j.exger.2018.10.003. Epub 2018 Oct 6. PMID: 30300667; PMCID: PMC6224709.

Goya, F. Xue, C. Sampedro-Torres-Quevedo, S. Arnaouteli, L. Riquelme-Dominguez, A. Romanowski, J. Brydon, K.L. Ball, N.R. Stanley-Wall, M. Doitsidou Probiotic Bacillus subtilis protects against alpha-synuclein aggregation in C. elegans Cell Rep., 30 (2020), pp. 367-380.e7

Hartler J, Trotzmuller M, Chitraju C, Spener F, Kofeler HC, Thallinger GG. Lipid Data Analyzer: unattended identification and quantitation of lipids in LC-MS data. Bioinformatics. 2011 Feb 15;27(4):572–7. Pmid:21169379

Hijioka M, Inden M, Yanagisawa D, Kitamura Y. DJ-1/PARK7: A New Therapeutic Target for Neurodegenerative Disorders. Biol Pharm Bull. 2017;40(5):548-552. doi: 10.1248/bpb.b16-01006. PMID: 28458339.

Hussain G, Anwar H, Rasul A, Imran A, Qasim M, Zafar S, Imran M, Kamran SKS, Aziz N, Razzaq A, Ahmad W, Shabbir A, Iqbal J, Baig SM, Ali M, Gonzalez de Aguilar JL, Sun T, Muhammad A, Muhammad Umair A. Lipids as biomarkers of brain disorders. Crit Rev Food Sci Nutr. 2020;60(3):351-374. doi: 10.1080/10408398.2018.1529653. Epub 2019 Jan 7. PMID: 30614244.

Kaletta, T., Hengartner, M. Finding function in novel targets: *C. elegans* as a model organism. *Nat Rev Drug Discov* 5, 387–399 (2006). https://doi.org/10.1038/nrd2031

Kamath, R., & Ahringer, J. (2003). Genome-wide RNAi screening in Caenorhabditis elegans. Methods, 30(4), 313-321. doi:10.1016/s1046-2023(03)00050-1

Kang UJ, Boehme AK, Fairfoul G, Shahnawaz M, Ma TC, Hutten SJ, Green A, Soto C. (2019). Comparative study of cerebrospinal fluid α-synuclein seeding aggregation assays for diagnosis of Parkinson's disease. Mov Disord. 34(4):536-544. doi: 10.1002/mds.27646. Epub 2019 Mar 6. PMID: 30840785; PMCID: PMC6519150.

Knight AL, Yan X, Hamamichi S, Ajjuri RR, Mazzulli JR, Zhang MW, Daigle JG, Zhang S, Borom AR, Roberts LR, Lee SK, DeLeon SM, Viollet-Djelassi C, Krainc D, O'Donnell JM, Caldwell KA, Caldwell GA. The glycolytic enzyme, GPI, is a functionally conserved modifier of dopaminergic neurodegeneration in Parkinson's models. Cell Metab. 2014 Jul 1;20(1):145-57. doi: 10.1016/j.cmet.2014.04.017. Epub 2014 May 29. PMID: 24882066; PMCID: PMC4097176.

Lewis KT, Maddipati KR, Naik AR, Jena BP. Unique Lipid Chemistry of Synaptic Vesicle and Synaptosome Membrane Revealed Using Mass Spectrometry. ACS Chem Neurosci. 2017 Jun 21;8(6):1163-1169. doi: 10.1021/acschemneuro.7b00030. Epub 2017 Mar 2. PMID: 28244738.

Li, JQ., Tan, L. & Yu, JT. The role of the LRRK2 gene in Parkinsonism. Mol Neurodegeneration 9, 47 (2014). https://doi.org/10.1186/1750-1326-9-47

Maulik, M., Mitra, S., Bult-Ito, A., Taylor, B. E., & Vayndorf, E. M. (2017). Behavioral Phenotyping and Pathological Indicators of Parkinson's Disease in C. elegans Models. Frontiers in genetics, 8, 77. https://doi.org/10.3389/fgene.2017.00077

Meneely PM, Dahlberg CL, Rose JK. (2019). Working with worms: Caenorhabditis elegans as a model organism. Cur Prot Essent Lab Tech. 2019;19:e35

Nair, A. T., Ramachandran, V., Joghee, N. M., Antony, S., & Ramalingam, G. (2018). Gut Microbiota Dysfunction as Reliable Non-invasive Early Diagnostic Biomarkers in the Pathophysiology of Parkinson's Disease: A Critical Review. Journal of neurogastroenterology and motility, 24(1), 30–42. https://doi.org/10.5056/jnm17105

Shahmoradian, S.H., Lewis, A.J., Genoud, C. et al. Lewy pathology in Parkinson's disease consists of crowded organelles and lipid membranes. Nat Neurosci 22, 1099–1109 (2019). https://doi.org/10.1038/s41593-019-0423-2

Sinclair, E., Trivedi, D.K., Sarkar, D. et al. (2021). Metabolomics of sebum reveals lipid dysregulation in Parkinson's disease.Nat Commun 12, 1592. https://doi.org/10.1038/s41467-021-21669-4

Schneider, S.A., Alcalay, R.N. (2020). Precision medicine in Parkinson's disease: emerging treatments for genetic Parkinson's disease. J Neurol 267, 860–869. https://doi.org/10.1007/s00415-020-09705-7

Su, X.Q., Wang, J. & Sinclair, A.J. Plasmalogens and Alzheimer's disease: a review. Lipids Health Dis 18, 100 (2019). https://doi.org/10.1186/s12944-019-1044-1

Sultana, N., & Olsen, C. P. (2020). Using stable isotope tracers to monitor membrane dynamics in C. elegans. Chemistry and Physics of Lipids, 233, 104990. doi:10.1016/j.chemphyslip.2020.104990

Spillantini M.G. , Crowther R.A., Jakes R. , Hasegawa M., & Goedert M. (1998). alpha-Synuclein in filamentous inclusions of Lewy bodies from Parkinson's disease and dementia with lewy bodies, Proc. Natl. Acad. Sci. USA, 95, pp. 6469-6473

Todd W. Harris, Erika Hartwieg, H. Robert Horvitz, Erik M. Jorgensen; Mutations in Synaptojanin Disrupt Synaptic Vesicle Recycling. J Cell Biol 7 August 2000; 150 (3): 589–600. doi: https://doi.org/10.1083/jcb.150.3.589

Tysnes, OB., Storstein, A. Epidemiology of Parkinson's disease. J Neural Transm 124, 901–905 (2017). https://doi.org/10.1007/s00702-017-1686-y

van Meer G, Voelker DR, Feigenson GW. Membrane lipids: where they are and how they behave. Nature Reviews Molecular Cell Biology. 2008;9:112–124. doi: 10.1038/nrm2330.

Vanni S., Riccardi L., Palermo G., De Vivo M. (2019). Structure and dynamics of the acyl chains in the membrane trafficking and enzymatic processing of lipids. Acc. Chem. Res. 10.1021/acs.accounts.9b00134

Xicoy, H., Wieringa, B., & Martens, G. (2019). The Role of Lipids in Parkinson's Disease. Cells, 8(1), 27. https://doi.org/10.3390/cells8010027

Xie F, Chen S, Cen ZD, Chen Y, Yang DH, Wang HT, Zhang BR, Luo W. A novel homozygous SYNJ1 mutation in two siblings with typical Parkinson's disease. Parkinsonism Relat Disord. 2019 Dec;69:134-137. doi: 10.1016/j.parkreldis.2019.11.001. Epub 2019 Nov 5. PMID: 31751865.

Watts JL, Ristow M. (2017) Lipid and Carbohydrate Metabolism in Caenorhabditis elegans. Genetics. 207(2):413-446. doi: 10.1534/genetics.117.300106. PMID: 28978773; PMCID: PMC5629314.